Thermal Residual Stresses in Aluminium Matrix Composites

F. Teixeira-Dias and L.F. Menezes

Abstract It is well known that residual stresses strongly influence the behaviour of most materials and, in particular, of composite materials. This chapter presents one approach to the numerical determination of thermal residual stresses in metal matrix composites (MMC). The subject of residual stresses is introduced and the corresponding mathematical and constitutive models are described in detail. It is considered that the reinforcement material is elastic and that the metallic matrix may exhibit thermoelastic-viscoplastic behaviour. A progressive gradient based time-integration algorithm is described that leads to the implementation of the proposed constitutive models in a finite element analysis code. The corresponding variational formulation and discretisation into finite elements is also described. In order to guarantee stabilised convergence and to increase the precision of results, the authors also propose a time-step optimisation algorithm. All the formalisms are tested measuring the influence of the reinforcement volume fraction and cooling rate on the resulting residual stresses.

1 Introduction

Nowadays, metal matrix composite materials (MMC) are highly relevant materials in the scope of engineering applications mostly due to their mechanical properties and characteristics. In general terms, these materials often have very high specific stiffness, strength and low density. Most of the manufacturing processes associated

F. Teixeira-Dias (✉)
GRIDS–DAPS Division of Armour & Protection Systems, Department of Mechanical Engineering, Universidade de Aveiro, Campus Universitário de Santiago, 3810-193 Aveiro, Portugal
e-mail: ftd@ua.pt

L.F. Menezes
Department of Mechanical Engineering, Universidade de Coimbra, 3030 Coimbra, Portugal
e-mail: luis.menezes@dem.uc.pt

A. Öchsner and G.E. Murch (eds.), *Heat Transfer in Multi-Phase Materials,*
Adv Struct Mater 2, DOI 10.1007/8611_2010_1,

to MMC imply that the material must, at some stage, go through high temperatures and temperature gradients. These temperatures are most of the time close, or even above, the melting temperature of the metallic matrix material. This fact determines most of the mechanical properties of the final material. Consequently, it is of utmost importance that adequate numerical methods and models are developed that can represent the behaviour of MMC over the whole temperature range. Additionally, due to the fact that the constituent materials will have distinct coefficients of thermal expansion (CTE) and their constitutive behaviour will be different it is possible that residual stresses may arise when the MMC is subjected to high amplitude temperature changes. These residual stresses (and consequent residual strains) will affect the final properties and behaviour of the MMC [1–8].

The high specific stiffness and strength of metal matrix composite materials, and their thermal properties are good enough reasons to justify the high strategic interest in these engineering materials. Presently there is a wide variety of modelling approaches to the behaviour of MMC. Most approaches are based on the distinct properties of the constituent materials – the matrix and the reinforcement materials [9–11]. Most of these models are micromechanical models and are thus also based on the topology and geometrical distribution of the reinforcement components.

The overall behaviour of a metal matrix composite material is often dependent on the temperature and is highly sensitive to its variations. This is due to two main reasons: (1) the behaviour of the metallic matrix is temperature dependent and (2) temperature changes induce residual stress and strain fields within the MMC, due to the mismatch of coefficients of thermal expansion [12, 13]. Nonetheless, residual stresses in MMC may also have a mechanical origin: these stresses may be due to the non-homogeneous flow of matrix material around the reinforcement elements.

In general terms, metallic materials used as matrix in metal matrix composites have coefficients of thermal expansion that are often one order of magnitude higher than the CTE of the ceramic reinforcement material. It is then predictable that when cooling down the MMC from fabrication temperature thermal residual stress fields may arise [14, 15].

2 Mathematical Modelling and Algorithms

The following paragraphs introduce the continua kinematics approach used to describe the thermal and mechanical behaviour of metal matrix composites. The constitutive models used for both MMC constituent materials are also presented and detailed. The section ends with a description of the time-integration procedures.

2.1 Constitutive Modelling

When a multiphase material is submitted to changes in temperature residual stress fields may be generated. These may be generated by the differences in the

coefficients of thermal expansion (CTE) of the constituent materials. The behaviour of materials under these conditions has been studied by many researchers often using experimental techniques [16–27].

2.1.1 Continua Kinematics

Within this text, an updated Lagrangian approach is proposed in order to continuously follow the evolution and movement of all material points in a particular medium. The goal is to determine the present configuration of the material, $\mathcal{C}_t$, starting from the reference configuration on a previous instant, $\mathcal{C}_0$. Let P be a material point in the continuous medium Ω and $\mathbf{p}$ and $\mathbf{x}$ the position vectors of this material point in the configurations $\mathcal{C}_0$ and $\mathcal{C}_t$, respectively, then

$$\mathbf{p} = \bar{\mathbf{p}}(\mathbf{x}, t), \tag{1}$$

$$\mathbf{x} = \bar{\mathbf{x}}(\mathbf{p}, t), \tag{2}$$

$$\mathbf{x} = \mathbf{p} + \mathbf{u}(\mathbf{p}, t), \tag{3}$$

where $\mathbf{u}(\mathbf{p}, t)$ represents the displacement of the material point P between the configurations $\mathcal{C}_0$ and $\mathcal{C}_t$. The gradient $\mathbf{F}$ of the point transformation $\mathbf{x}$ can be defined as:

$$\mathbf{F}(\mathbf{p}, t) = \mathbf{F} \doteq \frac{\partial}{\partial \mathbf{p}} \bar{\mathbf{x}}(\mathbf{p}, t) = \mathbf{I} + \frac{\partial}{\partial \mathbf{p}} \mathbf{u}(\mathbf{p}, t), \tag{4}$$

where $\mathbf{I}$ is the second order identity tensor. The velocity field associated with this transformation is

$$\dot{\bar{\mathbf{x}}}(\mathbf{p}, t) = \dot{\bar{\mathbf{x}}}(\bar{\mathbf{p}}(\mathbf{x}, t), t) \doteq \frac{\partial}{\partial t} \bar{\mathbf{x}}(\mathbf{p}, t) \tag{5}$$

to which corresponds the velocity gradient $\mathbf{L}$, defined as

$$\mathbf{L}(\mathbf{x}, t) \doteq \text{grad}[\mathbf{v}(\mathbf{x}, t)] = \frac{\partial}{\partial \mathbf{x}} \mathbf{v}(\mathbf{x}, t) = \frac{\partial}{\partial \mathbf{p}} \dot{\bar{\mathbf{x}}}(\mathbf{p}, t) \frac{\partial}{\partial \mathbf{x}} \bar{\mathbf{p}}(\mathbf{x}, t) \tag{6}$$

where grad is the gradient operator relative to $\mathbf{x}$, keeping t constant. According to (4), the previous relation can also be written as

$$\mathbf{L} = \dot{\mathbf{F}} \mathbf{F}^{-1}. \tag{7}$$

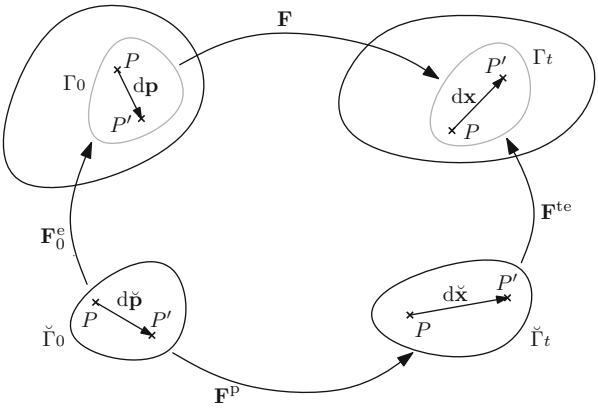

Fig. 1 Schematic representation of the decomposition of transformation gradient **F**

From this point it is important to distinguish the thermoelastic and viscoplastic contributions to the transformation gradient **F**, between instants t_0 and t. In order to do this one must analyse the infinitesimal neighbourhoods of material point P in both configurations $\mathcal{C}_0$ and $\mathcal{C}_0$, as shown in Fig. 1. The following configurations must also be defined: Γ_0 – the configuration of the infinitesimal neighbourhood of P at instant t_0; $\breve{\Gamma}_0$ – the configuration obtained after elastic relaxation of Γ_0; Γ_t – the configuration of the infinitesimal neighbourhood of P at instant t; and $\breve{\Gamma}_t$ – the configuration obtained after elastic relaxation of Γ_t.

Let d**p** be the position vector of material point P', in the infinitesimal neighbourhood of P, relative to P itself. Consequently, d$\breve{\mathbf{p}}$, d**x** and d$\breve{\mathbf{x}}$ are the transformations of vector d**p** within the configurations $\breve{\Gamma}_0$, Γ_t and $\breve{\Gamma}$, respectively. Thus, the following three transformation gradients can be defined in the neighbourhood of P: $\mathbf{F}^{\mathrm{e}}_0$ – the transformation gradient $\breve{\Gamma}_0$; $\mathbf{F}^{\mathrm{p}}$ – the transformation gradient $\breve{\Gamma}_0$; and $\mathbf{F}^{\mathrm{te}}$ – the transformation gradient $\breve{\Gamma}_t$. It is now possible to relate vectors d**p** and d**x** based on these definitions, that is,

$$\mathrm{d}\mathbf{x} = \mathbf{F}^{\mathrm{te}}\mathbf{F}^{\mathrm{p}}(\mathbf{F}^{\mathrm{e}}_0)^{-1}\mathrm{d}\mathbf{p}. \tag{8}$$

Relating the previous equation to (4) gradient **F** can be redefined as

$$\mathbf{F} = \mathbf{F}^{\mathrm{te}}\mathbf{F}^{\mathrm{p}}(\mathbf{F}^{\mathrm{e}}_0)^{-1}. \tag{9}$$

Replacing **F** in (7) it is possible to obtain

$$\mathbf{L} = \dot{\mathbf{F}}^{\mathrm{te}}(\mathbf{F}^{\mathrm{te}})^{-1} + \mathbf{F}^{\mathrm{te}}\dot{\mathbf{F}}^{\mathrm{p}}(\mathbf{F}^{\mathrm{p}})^{-1}(\mathbf{F}^{\mathrm{te}})^{-1} = \mathbf{L}^{\mathrm{te}} + \mathbf{L}^{\mathrm{p}}, \tag{10}$$

where $\mathbf{L}^{\mathrm{te}} = \dot{\mathbf{F}}^{\mathrm{te}}(\mathbf{F}^{\mathrm{te}})^{-1}$ and $\mathbf{L}^{\mathrm{p}} = \mathbf{F}^{\mathrm{te}}\dot{\mathbf{F}}^{\mathrm{p}}(\mathbf{F}^{\mathrm{p}})^{-1}(\mathbf{F}^{\mathrm{te}})^{-1}$ are the thermoelastic and viscoplastic parts of the velocity gradient tensor $\mathbf{L}$, respectively. However, $\mathbf{L}$ can still be decomposed to its strain rate ($\mathbf{D}$) and rotation rate ($\mathbf{W}$) tensors [28], as

$$\mathbf{L} = \mathbf{D} + \mathbf{W}. \tag{11}$$

These tensors correspond to the symmetric ($\mathbf{L}^{\mathrm{S}}$) and anti-symmetric ($\mathbf{L}^{\mathrm{A}}$) parts of $\mathbf{L}$, that is,

$$\mathbf{D}(\mathbf{x}, t) \doteq \mathbf{L}^{\mathrm{S}} = \frac{1}{2}\left(\mathbf{L} + \mathbf{L}^{\mathrm{T}}\right), \tag{12}$$

$$\mathbf{W}(\mathbf{x}, t) \doteq \mathbf{L}^{\mathrm{A}} = \frac{1}{2}\left(\mathbf{L} - \mathbf{L}^{\mathrm{T}}\right). \tag{13}$$

2.1.2 Material Behaviour

The goal of this text is to model the development of residual stresses in metal matrix composites (MMC). These stress fields can arise, for example, from the cooling down stage that is imposed on the MMC during the manufacturing process. Let $\dot{T}$ be the cooling rate, considered constant. It will also be assumed that the temperature field $T(t)$ is homogeneous within the material. Its evolution can then be described by

$$T(t) = T_0 + \dot{T}t. \tag{14}$$

T_0 is the initial temperature value, at time instant $t = t_0$. The material is considered to be stress free at $t = t_0$, which is a reasonable consideration due to the manufacturing temperatures of most metal matrix composites [29]. In technological processes involving the cooling down of two or more distinct materials (e.g. reinforcement and matrix) it is important to distinguish each behaviour model. This distinction will be made relating the melting (decomposition) temperature of each material (T^{m}) and the process temperature. This relation is designated by homologous temperature (T^{h}) and can be defined as

$$T^{\mathrm{h}} = \frac{T}{T^{\mathrm{m}}}. \tag{15}$$

2.1.3 Constitutive Modelling of the Reinforcement

The maximum temperature levels reached during the manufacturing processes of most MMCs are much lower than the decomposition temperature of the

reinforcement materials, thus the homologous temperature is often $T^{\mathrm{h}} < 1$. Facing this it is reasonable to consider that the reinforcement material exhibits thermo-elastic behaviour. As a consequence, the following hypotheses are assumed [30]: (1) elastic strains are small; (2) elastic behaviour is isotropic; and (3) the influence of plastic strain on the elastic constants can be neglected. The reinforcement behaviour can then be described by Hooke's hyperelastic law [31], i.e.

$$\dot{\sigma} = \mathbf{C}_{\mathrm{R}}^{\mathrm{e}} : \mathbf{D}^{\mathrm{e}}, \tag{16}$$

where $\dot{\sigma}$ is the time derivative of Cauchy's stress tensor and $\mathbf{C}_{\mathrm{R}}^{\mathrm{e}}$ is the elastic tensor of the reinforcement material which, assuming isotropic behaviour, can be defined as [32]

$$\mathbf{C}_{\mathrm{R}}^{\mathrm{e}} = 2\mu_{\mathrm{R}}\mathbf{1} + \lambda_{\mathrm{R}}\mathbf{I} \otimes \mathbf{I}, \tag{17}$$

where $\mathbf{1}$ is the fourth order identity tensor. μ_{R} and λ_{R} are Lamé's coefficients for the reinforcement material and $\mathbf{D}^{\mathrm{e}}$ is the elastic part of the thermoelastic strain rate tensor, given by

$$\mathbf{D}^{\mathrm{te}} = \mathbf{D}^{\mathrm{e}} + \mathbf{D}^{\mathrm{t}}. \tag{18}$$

The thermal part of the strain rate tensor is $\mathbf{D}^{\mathrm{t}} = \alpha_{\mathrm{R}}\dot{T}\,\mathbf{I}$ and α_{R} is the thermal expansion coefficient of the reinforcement. Combining and manipulating (16)–(18) it can be determined that

$$\dot{\sigma} = 2\mu_{\mathrm{R}}\mathbf{D}^{\mathrm{te}} + \left[\left(k_{\mathrm{R}} - \frac{2}{3}\mu_{\mathrm{R}}\right)\mathrm{trace}(\mathbf{D}^{\mathrm{te}}) - 3k_{\mathrm{R}}\alpha_{\mathrm{R}}\dot{T}\right]\mathbf{I}, \tag{19}$$

with

$$k_{\mathrm{R}} = \lambda_{\mathrm{R}} + \frac{2}{3}\mu_{\mathrm{R}}. \tag{20}$$

2.1.4 Constitutive Modelling of the Matrix

The maximum temperature reached during the manufacturing process of the MMC is often of the same order of magnitude as the melting temperature of the matrix material. For this reason the matrix homologous temperature is $T^{\mathrm{h}} \approx 1$. It is then admitted that the material behaviour is both temperature and strain rate dependent. Several constitutive models have been proposed for such situations. However, the authors will focus on a material model that uses an internal state variable that will allow the description of the static and dynamic recovery of the matrix material.

This model is developed based on the assumptions that plastic strains are highly dependent on the strain rate and that the internal state of the material determines its behaviour. The proposed model will allow the modelling of phenomena such as: (1) the effects of strain rate and temperature; (2) static and dynamic recovery and recrystallisation processes; (3) internal damage and its evolution; and (4) crystalline structure and its evolution.

When formulating the constitutive model it is necessary to identify the internal state variables. The proposed approach uses only one internal state variable, s, representing the resistance to plastic flow. This is clearly a limiting approach but it is nonetheless possible to model both hardening and sensitivity to strain rate and temperature with such a law [33]. The proposed model is based on the following decomposition of the strain rate tensor:

$$\mathbf{D} = \mathbf{D}^{\mathrm{e}} + \mathbf{D}^{\mathrm{t}} + \mathbf{D}^{\mathrm{vp}}, \tag{21}$$

where $\mathbf{D}^{\mathrm{e}}$ and $\mathbf{D}^{\mathrm{t}} = \alpha_{\mathrm{M}}\dot{T}\,\mathbf{I}$ are the elastic and thermal parts of the strain rate tensor, respectively. α_{M} is the temperature dependent thermal expansion coefficient of the matrix material. $\mathbf{D}^{\mathrm{vp}}$ is the viscoplastic strain rate tensor considered to be isochoric, that is, $\mathrm{trace}(\mathbf{D}^{\mathrm{vp}}) = 0$.

In the technological processes to be modelled it can be considered that strains are small when compared to 1 and that rotations can be neglected. Thus, the small strains approach is used and the evolution law of Cauchy's stress tensor is considered identical to the reinforcement material law, that is,

$$\dot{\sigma} = \mathbf{C}^{\mathrm{e}}_{\mathrm{M}} : \mathbf{D}^{\mathrm{e}}, \tag{22}$$

where the evolution of the material tensor $\mathbf{C}^{\mathrm{e}}_{\mathrm{M}}$ will be described by

$$\dot{\sigma} = 2\mu_{\mathrm{M}}(\mathbf{D} - \mathbf{D}^{\mathrm{vp}}) + \left[\left(k_{\mathrm{M}} - \frac{2}{3}\mu_{\mathrm{M}}\right)\mathrm{trace}(\mathbf{D}) - 3k_{\mathrm{M}}\alpha_{\mathrm{M}}\dot{T}\right]\mathbf{I}. \tag{23}$$

Lamé's coefficients for the matrix material are temperature dependent, i.e., $\mu_{\mathrm{M}} = \mu_{\mathrm{M}}(T)$ and $\lambda_{\mathrm{M}} = \lambda_{\mathrm{M}}(T)$. The constitutive relation for $\mathbf{D}^{\mathrm{vp}}$, or flow law, is described by [33]

$$\mathbf{D}^{\mathrm{vp}} = \frac{3\dot{\bar{\varepsilon}}^{\mathrm{p}}}{2\bar{\sigma}}\sigma'. \tag{24}$$

In the previous relation, σ' is Cauchy's stress deviatoric tensor and $\bar{\sigma}$ is von Mises' equivalent stress. The equivalent plastic strain rate, $\dot{\bar{\varepsilon}}^{\mathrm{p}}$, is

$$\dot{\bar{\varepsilon}}^{\mathrm{p}} = f(\bar{\sigma}, s, T). \tag{25}$$

It is necessary to define the function governing the evolution of the internal state variable s. This function is itself dependent on $\bar{\sigma}$, s and T, that is,

$$\dot{s} = g(\bar{\sigma}, s, T). \tag{26}$$

The state variable in (25) can be directly related to the equivalent stress in such a way that

$$\dot{\bar{\varepsilon}}^{\mathrm{p}} = f(\frac{\bar{\sigma}}{s}, T). \tag{27}$$

This condition agrees with previous dislocation slipping activation models [34]. It is also assumed that the evolution of the internal state variable can be defined by [35–37]

$$\dot{s} = g(\bar{\sigma}, s, T) = \dot{\bar{\varepsilon}}^{\mathrm{p}} h(\bar{\sigma}, s, T) - \dot{r}(s, T). \tag{28}$$

In this equation, $h(\bar{\sigma}, s, T)$ is associated with the hardening and dynamic restoration phenomena. Static restoration phenomena are described by $\dot{r}(s, T)$.

The independence of function $\dot{r}(s, T)$ from the equivalent stress reflects the fact that this function represents phenomena occurring within the material in the absence of applied stress. After experimental analyses it can be concluded that different materials have distinct functional dependences of $h(\bar{\sigma}, s, T)$ and $\dot{r}(s, T)$. Experimental tests done on aluminium show that a power law is the most adequate. As for Fe-2%Si the best dependence of the strain rate with the stress is exponential. Based on these observations the following combined exponential and power dependence between strain rate and stress can be stated:

$$\dot{\bar{\varepsilon}}^{\mathrm{p}} = A \exp\left(-\frac{Q}{R_g T}\right) \left[\sinh\left(\xi \frac{\sigma}{\mathrm{s}}\right)\right]^{1/m}, \tag{29}$$

where A, Q, m and ξ are material constants: A is the pre-exponential factor, m is the strain rate sensitivity, Q is the activation energy and R_g is the perfect gas constant. A relevant consequence of (29) is the proportional relation between the internal variable s and the equivalent stress $\bar{\sigma}$, that is, $\bar{\sigma} = cs$ where

$$c = \frac{1}{\xi} \sinh^{-1}\left\{\left[\frac{\dot{\bar{\varepsilon}}^{\mathrm{p}}}{A} \exp\left(\frac{Q}{R_g T}\right)\right]^m\right\}. \tag{30}$$

With the previous relation it is now possible to indirectly determine variable s. The proportionality between s and $\bar{\sigma}$ can be used to determine the static restoration function $\dot{r}(s, T)$ and the hardening function $h(\bar{\sigma}, s, T)$. However, previous experimental studies have proved that the influence of static restoration phenomena on the strain resistance is less than 1% of the overall strain resistance. Based on these

results, $\dot{r}(s,T)$ will be neglected on the following considerations. The adopted form for the hardening function is

$$h(\bar{\sigma},s,T) = h_0\left|1-\frac{s}{s^*}\right|^a \operatorname{sgn}\left(1-\frac{s}{s^*}\right) \tag{31}$$

with $a > 1$. Introducing (31) in relation (28) results in

$$\dot{s} = \dot{\bar{\varepsilon}}^{\mathrm{p}}\left[h_0\left|1-\frac{s}{s^*}\right|^a \operatorname{sgn}\left(1-\frac{s}{s^*}\right)\right] \tag{32}$$

where h_0 is the hardening rate and s^* is a saturation value for the scalar variable s, associated with a determined temperature and strain rate, such that

$$s^* = \bar{s}\left[\frac{\dot{\bar{\varepsilon}}^{\mathrm{p}}}{A}\exp\left(\frac{Q}{R_g T}\right)\right]^n. \tag{33}$$

The constants h_0, a, $\bar{s}$ and n are once more material parameters.

2.2 Time-Integration of the Constitutive Model

Differential equations describing the evolution of state variables of most physical processes with identical complexity of the ones described in this text can only be integrated numerically [38]. Several numerical integration approaches can be used with strain rate constitutive laws. These integration methods are often referred to as: (1) totally explicit or progressive methods; (2) totally implicit or regressive methods; or (3) semi-implicit or progressive gradient methods.

The constitutive relations used herein are numerically stable. However, when using a fully explicit Euler-type time integration scheme it is often necessary to significantly reduce the time step in order to guarantee numerical stability [35]. Using a semi-implicit integration algorithm is one way to overcome this question. These algorithms approximate the fully-implicit methods using Taylor series' developments of the constitutive functions and tolerate significantly larger time-steps [16]. The most relevant disadvantage of the progressive gradient methods is the fact that their precision deteriorates when large time increments are used in high gradient stages of the simulation. As a consequence, it is necessary to associate careful time-step control algorithms with these integration procedures [28, 38].

2.2.1 Progressive Gradient Integration Method

The set of constitutive equations proposed here has, among other, the advantage of using a scalar parameter s that represents the internal state of the material and

models the resistance of the material to plastic flow. The time integration of these equations can be made with a progressive gradient integration method [28, 39].

The main goal of the integration method is to determine the configuration $\mathcal{C}_{n+1}$ starting from the initial step configuration $\mathcal{C}_n$, at a time interval Δt. The known state variables at $\mathcal{C}_n$ are σ_n, s_n and T_n. The state variables at $\mathcal{C}_{n+1}$ are σ_{n+1}, s_{n+1} and T_{n+1}. The first step is to integrate the viscoplastic strain rate tensor $\mathbf{D}^{\text{vp}}$ along the time increment Δt in order to determine the plastic strain increment $\Delta\varepsilon^{\text{p}}$, that is,

$$\Delta\varepsilon^{\text{p}} = \int_{t_n}^{t_{n+1}} \mathbf{D}^{\text{vp}} \mathrm{d}t. \tag{34}$$

This integration can be made using the approximation

$$\Delta\varepsilon^{\text{p}} = \bar{\mathbf{D}}^{\text{vp}} \Delta t \tag{35}$$

where $\bar{\mathbf{D}}^{\text{vp}}$ is the viscoplastic strain rate tensor weighted from the limit time instants of the increment, that is,

$$\bar{\mathbf{D}}^{\text{vp}} = \mathbf{D}_n^{\text{vp}} + \Phi\left(\mathbf{D}_{n+1}^{\text{vp}} - \mathbf{D}_n^{\text{vp}}\right). \tag{36}$$

Φ is a scalar parameter defined in the interval [0, 1] and represents the weighting factor for the integration. $\mathbf{D}_{n+1}^{\text{vp}}$ is determined using a first order truncated Taylor approximation in such a way that

$$\mathbf{D}_{n+1}^{\text{vp}} = \mathbf{D}_n^{\text{vp}} + \frac{\partial \mathbf{D}_n^{\text{vp}}}{\partial f}\Delta f + \frac{\partial \mathbf{D}_n^{\text{vp}}}{\partial \bar{\sigma}}\Delta\bar{\sigma} + \frac{\partial \mathbf{D}_n^{\text{vp}}}{\partial \sigma'}\Delta\sigma'. \tag{37}$$

Performing the partial derivatives in the previous relation leads to

$$\mathbf{D}_{n+1}^{\text{vp}} = \frac{3f_n}{2\bar{\sigma}}\sigma'_n + \frac{3\sigma'_n}{2\bar{\sigma}_n}\Delta f + \frac{3}{2}f_n\sigma'_n\left(-\frac{1}{\bar{\sigma}_n^2}\right)\Delta\bar{\sigma} + \frac{3f_n}{2\bar{\sigma}_n}\Delta\sigma'. \tag{38}$$

where the equivalent viscoplastic strain increment is the increment of the function $f(\bar{\sigma}, s, T)$, that is,

$$\Delta f = \frac{\partial f_n}{\partial \bar{\sigma}}\Delta\bar{\sigma} + \frac{\partial f_n}{\partial s}\Delta s + \frac{\partial f_n}{\partial T}\Delta T \tag{39}$$

and the equivalent stress increment is

$$\Delta\bar{\sigma} = \frac{\partial\bar{\sigma}}{\partial\sigma'} : \Delta\sigma'. \tag{40}$$

Performing the derivatives with respect to σ' one obtains

$$\frac{\partial \bar{\sigma}}{\partial \sigma'} = \frac{1}{2}\left(\frac{3}{2}\sigma'_n : \sigma'_n\right)^{-1/2}(3\sigma'_n) = \frac{3}{2\bar{\sigma}_n}\sigma'_n. \tag{41}$$

Introducing the previous relation in (40) results in

$$\Delta\bar{\sigma} = \frac{3}{2\bar{\sigma}_n}\sigma'_n : \Delta\sigma'. \tag{42}$$

In order to determine the increment of the deviatoric Cauchy stress tensor, $\Delta\sigma'$, it is first necessary to calculate the deviatoric part of the stress rate tensor $\dot{\sigma}$. Introducing tensor $\dot{\sigma}$ and calculating its deviatoric part results in

$$\dot{\sigma}' = 2\mu_{\mathrm{M}}\left(\mathbf{D}' - \mathbf{D}^{\mathrm{vp}}\right). \tag{43}$$

Integrating along Δt the increment of the deviatoric Cauchy stress tensor becomes

$$\Delta\sigma' = 2\mu_{\mathrm{M}}(\Delta\varepsilon' - \Delta\varepsilon^{\mathrm{p}}), \tag{44}$$

where the total strain increment and its deviatoric part are

$$\Delta\varepsilon = \int_{t_n}^{t_n+\Delta t} \mathbf{D}\mathrm{d}t \quad \text{and} \quad \Delta\varepsilon' = \Delta\varepsilon - \frac{1}{3}\mathrm{trace}(\Delta\varepsilon)\mathbf{I}, \tag{45}$$

respectively. Manipulating relations (35)–(38) it is possible to derive the following relation to determine the plastic strain increment:

$$\Delta\varepsilon^{\mathrm{p}} = \left(\frac{3\sigma'_n}{2\bar{\sigma}_n}\right)\left[f_n + \Phi\left(\frac{\partial f_n}{\partial\bar{\sigma}}\Delta\bar{\sigma} + \frac{\partial f_n}{\partial s}\Delta s + \frac{\partial f_n}{\partial T}\Delta T\right)\right]\Delta t \tag{46}$$

$$+ \Phi\frac{3f_n}{2\bar{\sigma}_n}\left[\Delta\sigma' - \left(\sigma'_n : \Delta\sigma'\right)\frac{3\sigma'_n}{2\bar{\sigma}_n^2}\right]\Delta t, \tag{47}$$

or, in a more compact form

$$\Delta\varepsilon^{\mathrm{p}} = \Delta\bar{\varepsilon}^{\mathrm{p}}\left(\frac{3\sigma'_n}{2\bar{\sigma}_n}\right) + \frac{3}{2h_1}\left[\Delta\sigma' - \left(\sigma'_n : \Delta\sigma'\right)\frac{3\sigma'_n}{2\bar{\sigma}_n^2}\right], \tag{48}$$

where the scalar h_1 is

$$h_1 = \frac{\bar{\sigma}_n}{\Phi f_n \Delta t} \tag{49}$$

and the equivalent plastic strain increment is

$$\Delta\bar{\varepsilon}^{\mathrm{p}} = \left[f_n + \Phi \left(\frac{\partial f_n}{\partial \bar{\sigma}} \Delta\bar{\sigma} + \frac{\partial f_n}{\partial s} \Delta s + \frac{\partial f_n}{\partial T} \Delta T \right) \right] \Delta t. \tag{50}$$

Performing the scalar product between the deviatoric stress tensor σ'_n and the plastic strain increment $\Delta\varepsilon^{\mathrm{p}}$, defined in (48), leads to

$$\sigma'_n : \Delta\varepsilon^{\mathrm{p}} = \Delta\bar{\varepsilon}^{\mathrm{p}} \left(\frac{3\sigma'_n : \sigma'_n}{2\bar{\sigma}_n} \right) + \frac{3}{2h_1} \left[\sigma'_n : \Delta\sigma' - \left(\sigma'_n : \Delta\sigma' \right) \frac{3\sigma'_n : \sigma'_n}{2\bar{\sigma}_n^2} \right]. \tag{51}$$

Combining relations (42) and (44) it is possible to derive the following expression for the equivalent stress increment:

$$\Delta\bar{\sigma} = \frac{3\mu_{\mathrm{M}}}{\bar{\sigma}_n} \sigma'_n : \Delta\varepsilon' - 3\mu_{\mathrm{M}} \Delta\bar{\varepsilon}^{\mathrm{p}}. \tag{52}$$

The scalar product $\sigma'_n : \Delta\varepsilon'$ can be simplified replacing σ'_n and $\Delta\varepsilon'$ by its definitions, that is,

$$\sigma'_n : \Delta\varepsilon' = \left[\sigma_n - \frac{1}{3} \mathrm{trace}(\sigma_n) \mathbf{I} \right] : \left[\Delta\varepsilon - \frac{1}{3} \mathrm{trace}(\Delta\varepsilon) \mathbf{I} \right] \tag{53}$$

leading to

$$\sigma'_n : \Delta\varepsilon' = \sigma_n : \Delta\varepsilon - \frac{1}{3} \mathrm{trace}(\sigma_n) \mathbf{I} : \Delta\varepsilon \quad \text{or} \quad \sigma'_n : \Delta\varepsilon' = \sigma'_n : \Delta\varepsilon. \tag{54}$$

Consequently, relation (52) can be rewritten in the form

$$\Delta\bar{\sigma} = \frac{3\mu_{\mathrm{M}}}{\bar{\sigma}_n} \sigma'_n : \Delta\varepsilon - 3\mu_{\mathrm{M}} \Delta\bar{\varepsilon}^{\mathrm{p}}. \tag{55}$$

Replacing the equivalent stress increment $\Delta\bar{\sigma}$ (55) in the formulation of the equivalent plastic strain increment (50), recalling that the increment of the internal state variable is $\Delta s = \Delta\bar{\varepsilon}^{\mathrm{p}} h$ and performing some algebraic manipulation leads to

$$\Delta\bar{\varepsilon}^{\mathrm{p}} = \frac{\Delta t}{1 + \nu_n} \left(f_n + \Phi \frac{3\mu_{\mathrm{M}}}{\bar{\sigma}_n} \frac{\partial f_n}{\partial \bar{\sigma}} \sigma'_n : \Delta\varepsilon + \Phi \frac{\partial f_n}{\partial T} \Delta T \right), \tag{56}$$

where the scalar variable v_n is

$$v_n = \Phi \frac{\partial f_n}{\partial \bar{\sigma}} G_n \Delta T \quad \text{with} \quad G_n = 3\mu_{\mathrm{M}} - h_n \left(\frac{\partial f_n}{\partial s} \Big/ \frac{\partial f_n}{\partial \bar{\sigma}} \right). \tag{57}$$

Inserting the deviatoric stress increment $\Delta\sigma'$, given by relation (44), in (48), that defines the plastic strain increment, results in

$$\Delta\varepsilon^{\mathrm{p}} = \Delta\bar{\varepsilon}^{\mathrm{p}} \left(\frac{3\sigma'_n}{2\bar{\sigma}_n} \right) + \frac{3}{2h_1} \left[2\mu_{\mathrm{M}} (\Delta\varepsilon' - \Delta\varepsilon^{\mathrm{p}}) - \frac{3\mu_{\mathrm{M}}}{\bar{\sigma}_n^2} \left(\sigma'_n : \Delta\sigma' \right) \sigma'_n \right]. \tag{58}$$

Finally replacing the deviatoric strain increment $\Delta\varepsilon'$ and rearranging all terms leads to

$$\begin{aligned} \Delta\varepsilon^{\mathrm{p}} = {} & \frac{3\bar{\mu}_n}{\mu_{\mathrm{M}}} \left(1 + \frac{3\mu_{\mathrm{M}}}{h_1} \right) \frac{\sigma'_n}{2\bar{\sigma}_n} \Delta\bar{\varepsilon}^{\mathrm{p}} + \frac{3\bar{\mu}_n}{h_1} \left[\Delta\varepsilon - \frac{1}{3} \mathrm{trace}(\Delta\varepsilon) \right] \\ & - \frac{9\bar{\mu}_n}{h_1 \bar{\sigma}_n^2} \left(\sigma'_n : \Delta\varepsilon \right) \sigma'_n, \end{aligned} \tag{59}$$

where

$$\bar{\mu}_n = \frac{\mu_{\mathrm{M}}}{1 + 3\mu_{\mathrm{M}}/h_1}. \tag{60}$$

2.2.2 Elasto-Plastic Secant Modulus

In order to determine the increment of the stress tensor it is necessary to integrate the previously defined constitutive law along the whole time increment $\Delta t \equiv [t_n, t_{n+1}]$, that is,

$$\dot{\sigma} = 2\mu_{\mathrm{M}} \mathbf{D} + \left(k_{\mathrm{M}} - \frac{2}{3}\mu_{\mathrm{M}} \right) \mathrm{trace}(\mathbf{D}) \mathbf{I} - 2\mu_{\mathrm{M}} \mathbf{D}^{\mathrm{vp}} - 3k_{\mathrm{M}} \alpha_{\mathrm{M}} \dot{T} \mathbf{I}. \tag{61}$$

Linearising the previous differential equation along the time increment Δt, replacing the plastic strain increment (59) and recalling relations (34) and (45), it is possible to obtain

$$\begin{aligned}\Delta\sigma = {} & 2\mu_{\mathrm{M}}\Delta\varepsilon - 2\bar{\mu}_n\left(\frac{3\sigma'_n}{2\bar{\sigma}_n}+\frac{9\bar{\mu}_n}{2h_1}\frac{\sigma'_n}{\bar{\sigma}_n}\right)\left[f_n+\Phi\left(\frac{3\mu_{\mathrm{M}}}{\bar{\sigma}_n}\frac{3\mu_{\mathrm{M}}}{\bar{\sigma}_n^2}\sigma'_n:\Delta\varepsilon\right)\frac{\partial f_n}{\partial\bar{\sigma}}\right.\\ & \left.+\Phi\frac{\partial f_n}{\partial T}\Delta T\right]\frac{\Delta t}{1+v_n}-2\bar{\mu}_n\frac{3\mu_{\mathrm{M}}}{h_1}\left[\Delta\varepsilon-\frac{1}{3}\mathrm{trace}(\Delta\varepsilon)\right]\\ & +2\bar{\mu}_n\frac{9\mu_{\mathrm{M}}}{2h_1\bar{\sigma}_n^2}\left(\sigma'_n:\Delta\varepsilon\right)\sigma'_n+\left(k_{\mathrm{M}}-\frac{2}{3}\mu_{\mathrm{M}}\right)\mathrm{trace}(\Delta\varepsilon)\mathbf{I}-3k_{\mathrm{M}}\alpha_{\mathrm{M}}(\Delta T)\mathbf{I}.\end{aligned} \tag{62}$$

or, in a more compact way,

$$\Delta\sigma = 2\mu_{\mathrm{M}}\Delta\varepsilon+\bar{\lambda}_n\ \mathrm{trace}(\Delta\varepsilon)\mathbf{I}-K_1\left(\sigma'_n:\Delta\varepsilon\right)\sigma'_n-K_2\sigma'_n-3k_{\mathrm{M}}\alpha_{\mathrm{M}}(\Delta T)\mathbf{I}. \tag{63}$$

In the previous relation

$$K_1=\frac{3}{\bar{\sigma}_n^2}\left[\frac{v_n}{1+v_n}\frac{3\mu_{\mathrm{M}}^2}{G_n}-(\mu_{\mathrm{M}}-\bar{\mu}_n)\right], \tag{64}$$

$$K_2=\frac{\Delta t}{1+v_n}\left(f_n+\Phi\frac{\partial f_n}{\partial T}\Delta T\right)\frac{3\mu_{\mathrm{M}}}{\bar{\sigma}_n}\ \text{and}\ \bar{\lambda}_n=k_{\mathrm{M}}-\frac{2}{3}\bar{\mu}_n. \tag{65}$$

Finally, performing some algebraic rearrangement of (63) leads to

$$\Delta\sigma=\mathbf{M}^{\mathrm{sec}}:\Delta\varepsilon-K_2\sigma'_n-3k_{\mathrm{M}}\alpha_{\mathrm{M}}(\Delta T)\mathbf{I}. \tag{66}$$

In the previous relation, $\mathbf{M}^{\mathrm{sec}}$ is the elasto-plastic secant modulus, that can be defined by its components as

$$M_{ijkl}^{\mathrm{sec}}=\bar{\lambda}_n\delta_{ij}\delta kl+\bar{\mu}_n(\delta_{ik}\delta jl+\delta_{il}\delta jk)-K_1\sigma'_{ij}\sigma'_{kl}, \tag{67}$$

where δ_{ij} is the Kronecker delta.

2.3 Variational Formulation and Discretisation

Performing numerical simulations using the finite element method (FEM) is essentially an approximation to determine the behaviour of a real system. This task can be done solving a limited set of equations that describe the real system.

2.3.1 Equilibrium Equations and Boundary Conditions

The system to be modelled is a solid deformable body that occupies a physical space designated by Ω delimited by an exterior surface Σ. As this work concerns metal matrix composites (MMC), Ω is built from zones from distinct materials, one

metallic – the metal matrix, Ω_M – and the other ceramic – the reinforcement, Ω_R. Ω can thus be defined by the following relations:

$$\Omega_R = \cup_i \Omega_R^i \text{ and } \Omega = \Omega_M \cup \Omega_R. \tag{68}$$

It is supposed that at time instant t, Ω is subjected to a set of diverse external loads: volume and surface loads, temperature variations, etc. The exterior surface of Ω is divided in a set of surfaces Σ_i such that $\Sigma = \cup_i \Sigma_i$ in which velocities and/or loads are known and prescribed. Thus, neglecting the effect of volumetric loads, it is possible to formulate the equilibrium of Ω as follows:

$$\text{div}\sigma = \mathbf{0}, \text{ in } \Omega. \tag{69}$$

The boundary conditions to which the deformable body Ω is subjected can also be listed as follows:

$$\mathbf{v} = \mathbf{v}^* \text{ on } \Sigma_v, \quad \mathbf{t} = \mathbf{t}^* \text{ on } \Sigma_t \quad \text{and} \quad \mathbf{v} = \mathbf{v}^* \wedge \mathbf{t} = \mathbf{t}^* \text{ on } \Sigma_{v,t} \tag{70}$$

where $\mathbf{v}$ and $\mathbf{v}^*$ are generic and prescribed velocities, respectively, and $\mathbf{t}$ and $\mathbf{t}^*$ are generic and prescribed Cauchy stress vectors, respectively. If $\mathbf{n}$ is the unit external normal vector that defines Σ, then $\mathbf{t} = \sigma\mathbf{n}$. Boundary conditions are considered to be unaltered during the whole duration of the process.

2.3.2 Variational Formulation

The generic problem defined by (69) and (70) is satisfied only on the condition that the principle of virtual work (PVW) is also satisfied whatever the virtual velocity field $\delta\mathbf{v}$, that is,

$$\int_\Omega \sigma : \delta\mathbf{D}\text{d}\Omega = \int_{\Sigma_t} \mathbf{t}^* \delta\mathbf{v}\text{d}\Sigma + \int_{\Sigma_{v,t}} \mathbf{t}^* \delta\mathbf{v}\text{d}\Sigma. \tag{71}$$

However, once this work concerns only the development of residual stresses in MMC due to the cooling down process, the effects of external loads are not considered. Consequently, the PVW becomes

$$\int_\Omega \sigma : \delta\mathbf{D}\text{d}\Omega = \mathbf{0}, \tag{72}$$

where $\delta\mathbf{D}$ is the symmetric part of the virtual velocity gradient tensor. The virtual velocity field is continuously differentiable and confines to the boundary conditions defined in Σ_v.

The principle of virtual work is written in two distinct forms: (1) total Lagrangian and (2) updated Lagrangian. On the first approach all integrations of the PVW are relative to the initial configuration of the system, $\mathcal{C}_0$. The updated Lagrangian approach is computationally more expensive because the integrations are performed relative to a reference configuration $\mathcal{C}_t$, which is the initial configuration of each time increment $[t, t + \Delta t]$. This last approach is the one adopted within this work and will be described on the following paragraphs.

The configuration of the deformable body Ω at time instant t is the reference configuration, $\mathcal{C}_0$, for the current time step $[t, t + \Delta t]$. The final configuration at the end of the current time increment, $\mathcal{C}$, is then the reference configuration for the next step. Thus, (72) becomes

$$\int_{\Omega(C_0)} \sigma_t : \delta\mathbf{D}\mathrm{d}\Omega = \mathbf{0}, \tag{73}$$

where σ_t is Cauchy's stress tensor at the start of the increment (instant t). Assuming that only small strains and rotations occur between two consecutive configurations it is possible to subtract the PVW from the initial and ending instant of the time step, resulting in

$$\int_{\Omega(C)} \sigma_{t+\Delta t} : \delta\mathbf{D}\mathrm{d}\Omega - \int_{\Omega(C_0)} \sigma_t : \delta\mathbf{D}\mathrm{d}\Omega = \mathbf{0}. \tag{74}$$

The previous relation can be simplified as

$$\int_{\Omega(C_0 \to C)} \Delta\sigma : \delta\mathbf{D}\mathrm{d}\Omega = \mathbf{0}. \tag{75}$$

2.3.3 Discretisation of the Principle of Virtual Work

The implementation of the principle of virtual work (PVW) with the finite element method (FEM) starts by performing the discretisation of the virtual strain rate tensor $\delta\mathbf{D}$, in the form

$$\delta\mathbf{D} = \frac{1}{2}\left\{\frac{\partial(\delta\mathbf{v})}{\partial\mathbf{x}_0} + \left[\frac{\partial(\delta\mathbf{v})}{\partial\mathbf{x}_0}\right]^{\mathrm{T}}\right\} \quad \text{or} \quad \delta\mathbf{D} = [\mathrm{grad}(\delta\mathbf{V})]^{\mathrm{S}}. \tag{76}$$

Once the deformable body Ω is discretised in finite elements the virtual velocity field $\delta\mathbf{v}$ is discretised as follows:

$$\delta\mathbf{v}(\mathbf{x}, t) = \sum_{A=1}^{NN} \mathbf{N}_A(\mathbf{x})\delta\mathbf{v}_A(t). \tag{77}$$

NN is the total number of nodes in the finite element mesh, $\mathbf{N}_A(\mathbf{x})$ are the shape functions and $\delta\mathbf{v}_A$ are the virtual velocities determined at the mesh nodes. Inserting the velocity field $\delta\mathbf{v}$ in relation (76) leads to

$$\delta\mathbf{D} = \left\{ \text{grad} \left[\sum_{A=1}^{NN} \mathbf{N}_A(\mathbf{x}) \delta\mathbf{v}_A(t) \right] \right\}^{\text{S}} = \sum_{A=1}^{NN} \mathbf{B}_A(\mathbf{x}) \delta\mathbf{v}_A(t), \tag{78}$$

where $\mathbf{B}_A(\mathbf{x})$ is the derivative of the shape function matrix.

Introducing the virtual strain rate tensor $\delta\mathbf{D}$ in the principle of virtual work, and after some algebraic manipulation, results in

$$\sum_{A=1}^{NN} \delta\mathbf{v}_A^{\text{T}} \int_{\Omega} \mathbf{B}_A^{\text{T}} \Delta\sigma \text{d}\Omega = \mathbf{0}. \tag{79}$$

Once the principle of virtual work is valid whatever the virtual velocity field $\delta\mathbf{v}_A$, (79) becomes

$$\int_{\Omega} \mathbf{B}_A^{\text{T}} \Delta\sigma \text{d}\Omega = \mathbf{0} = \mathbf{Q}_A \quad \text{with} \quad A = 1, \ldots, NN. \tag{80}$$

However, once the present work concerns sets of distinct materials, the stress increment $\Delta\sigma$ must be determined separately for $\mathbf{x} \in \Omega_{\text{R}}$ or $\mathbf{x} \in \Omega_{\text{M}}$. Consequently, the following two relations are valid distinctly for the two materials:

$$\mathbf{Q}_A^{\text{R}} = \int_{\Omega_{\text{R}}} \mathbf{B}_A^{\text{T}} \Delta\sigma_{\text{R}} \text{d}\Omega \quad \text{and} \quad \mathbf{Q}_A^{\text{M}} = \int_{\Omega_{\text{M}}} \mathbf{B}_A^{\text{T}} \Delta\sigma_{\text{M}} \text{d}\Omega. \tag{81}$$

2.3.4 Finite Elements

As an example, the deformable body Ω is discretised in isoparametric 8-node hexaedric elements with trilinear interpolation functions. This particular finite element has eight integration points for full integration and one for reduced integration [40, 41]. However, this isoparametric finite element has deficient behaviour when used to solve problems involving plastic strain [42, 43]. Using this finite element with full integration – using all the integration points – significantly increases the global stiffness of the element, leading to abnormal hydrostatic stresses and deteriorating the final solution. This particular phenomenon is associated with the fact that plastic strain is isochoric. Nonetheless, it is possible to

correct this by reducing the number of integration points used in each element. This technique is designated by uniform reduced integration.

The discretisation of the velocity and virtual velocity fields $\mathbf{v}$ and $\delta\mathbf{v}$, respectively, are given by

$$\mathbf{v} = \sum_{a=1}^{NE} \mathbf{N}_a^e \mathbf{v}_a^e \quad \text{and} \quad \delta\mathbf{v} = \sum_{a=1}^{NE} \mathbf{N}_a^e \delta\mathbf{v}_a^e. \tag{82}$$

$\mathbf{v}_a^e$ and $\delta\mathbf{v}_a^e$ on the previous relations are the nodal and virtual nodal velocities of node a, respectively. From relations (82) it is possible to write the velocity gradient tensor $\mathbf{L}$ and the virtual velocity gradient tensor $\delta\mathbf{L}$ as

$$\mathbf{L} = \frac{\partial \mathbf{v}}{\partial \mathbf{x}} = \sum_{a=1}^{NE} \frac{\partial \mathbf{N}_a^e}{\partial \mathbf{x}} \mathbf{v}_a^e \quad \text{and} \quad \delta\mathbf{L} = \frac{\partial (\delta\mathbf{v})}{\partial \mathbf{x}} = \sum_{a=1}^{NE} \frac{\partial \mathbf{N}_a^e}{\partial \mathbf{x}} \delta\mathbf{v}_a^e, \tag{83}$$

respectively. When using full integration, tensors $\mathbf{L}$ and $\delta\mathbf{L}$ are determined on all Gauss integration points. When using uniform reduced integration $\mathbf{L}$ and $\delta\mathbf{L}$ are calculated only on the reduced integration point – the center of the finite element. However, this technique leads to reduced stiffness, may lead to the appearance of eigenmodes and deteriorates the final solution. One way to avoid all these problems is to implement a reduced selective integration approach [44–47]. In the process, frequently designated by $\bar{\mathbf{B}}$, reduced integration is selectively applied only to some terms of the stiffness matrix. The hydrostatic components of tensors $\mathbf{L}$ and $\delta\mathbf{L}$ are considered constant within the whole element and are thus calculated only on the reduced integration point. For this purpose, $\mathbf{L}$ is decomposed on its deviatoric and hydrostatic components as

$$\mathbf{L} = \mathbf{L}' + \mathbf{L}^{\mathrm{h}} \quad \text{where} \quad \mathbf{L}^{\mathrm{h}} = \frac{1}{3}\mathrm{trace}(\mathbf{L})\mathbf{I}. \tag{84}$$

The tensor $\mathbf{L}$ can then be replaced by a tensor designated by $\bar{\mathbf{L}}$, such that

$$\bar{\mathbf{L}} = \mathbf{L} + \bar{\mathbf{L}}^{\mathrm{h}} - \mathbf{L}^{\mathrm{h}}, \tag{85}$$

and $\bar{\mathbf{L}}^{\mathrm{h}}$ is determined only on the central integration point. Thus, the discretisation of $\bar{\mathbf{L}}$ leads to

$$\bar{\mathbf{L}} = \sum_{a=1}^{NE} \left\{ \frac{\partial \mathbf{N}_a^e}{\partial \mathbf{x}} \mathbf{v}_a^e + \frac{1}{3} \left[\frac{\partial \mathbf{N}_a^e}{\partial \mathbf{x}} \mathrm{trace}\left(\mathbf{v}_a^e\right) - \frac{\partial \mathbf{N}_a^e}{\partial \mathbf{x}} \mathrm{trace}\left(\mathbf{v}_a^e\right) \right] \right\} \tag{86}$$

where $\bar{\mathbf{N}}_a^e$ corresponds to $\mathbf{N}_a^e$ determined at the central point of the finite element.

2.3.5 Element Equations

Integrating (19) along the whole time increment $[t, t+\Delta t]$ and considering relation (45) it becomes possible to determine the stress increment in the reinforcement material $\Delta\sigma_{\mathrm{R}}$, that is,

$$\Delta\sigma_{\mathrm{R}} = 2\mu_{\mathrm{R}}\Delta\varepsilon + \left[\left(k_{\mathrm{R}} - \frac{2}{3}\mu_{\mathrm{R}}\right)\mathrm{trace}(\Delta\varepsilon) - 3k_{\mathrm{R}}\alpha_{\mathrm{R}}(\Delta T)\right]\mathbf{I}. \tag{87}$$

After some algebraic manipulation the previous relation becomes

$$\Delta\sigma_{\mathrm{R}} = \mathbf{C}_{\mathrm{R}}^{e}\Delta\varepsilon - 3k_{\mathrm{R}}\alpha_{\mathrm{R}}(\Delta T)\mathbf{I} \tag{88}$$

where $\mathbf{C}_{\mathrm{R}}^{e}$, defined in (17), is time- and temperature-independent. Inserting the stress increment $\Delta\sigma_{\mathrm{R}}$ in the formulation of the principle of virtual work leads to

$$\mathbf{Q}_{a}^{\mathrm{R}} = \int_{\Omega_{\mathrm{R}}} \mathbf{B}_{a}^{\mathrm{T}}\left[\mathbf{C}_{\mathrm{R}}^{e}\Delta\varepsilon - 3k_{\mathrm{R}}\alpha_{\mathrm{R}}(\Delta T)\mathbf{I}\right]\mathrm{d}\Omega. \tag{89}$$

The discretisation of the incremental strain field $\Delta\varepsilon$ results in

$$\Delta\varepsilon = \sum_{b=1}^{NE}\mathbf{B}_{b}\Delta\mathbf{u}_{b}. \tag{90}$$

Introducing $\Delta\varepsilon$ given by the previous relation in expression (89) one obtains

$$\mathbf{Q}_{a}^{\mathrm{R}} = \sum_{b=1}^{NE}\left(\int_{\Omega_{\mathrm{R}}}\mathbf{B}_{a}^{\mathrm{T}}\mathbf{C}_{\mathrm{R}}^{e}\mathbf{B}_{b}\mathrm{d}\Omega\right)\Delta\mathbf{u}_{b} - 3k_{\mathrm{R}}\alpha_{\mathrm{R}}(\Delta T)\int_{\Omega_{\mathrm{R}}}\mathbf{B}_{a}^{\mathrm{T}}\mathbf{I}\mathrm{d}\Omega, \tag{91}$$

or, written in a compacted form,

$$\mathbf{Q}_{a}^{\mathrm{R}} = \mathbf{0} = \sum_{b=1}^{NE}\mathbf{k}_{ab}^{\mathrm{R}}\Delta\mathbf{u}_{b} - \Delta\mathbf{f}_{a}^{\mathrm{R}}. \tag{92}$$

Expression (92) is the generic equilibrium system of equations of a finite element of reinforcement material, where

$$\mathbf{k}_{ab}^{\mathrm{R}} = \int_{\Omega_{\mathrm{R}}}\mathbf{B}_{a}^{\mathrm{T}}\mathbf{C}_{\mathrm{R}}^{e}\mathbf{B}_{b}\mathrm{d}\Omega \quad \text{and} \quad \Delta\mathbf{f}_{a}^{\mathrm{R}} = 3k_{\mathrm{R}}\alpha_{\mathrm{R}}(\Delta T)\int_{\Omega_{\mathrm{R}}}\mathbf{B}_{a}^{\mathrm{T}}\mathbf{I}\mathrm{d}\Omega. \tag{93}$$

are the stiffness matrix and the second member for the reinforcement material finite elements, respectively.

According to previous sections, the matrix material exhibits thermoelastic-viscoplastic behaviour. Thus, the increments of plastic strain $\Delta\varepsilon^{\mathrm{p}}$ and stress $\Delta\sigma_{\mathrm{M}}$ were determined in Sect. 2.2.1. Inserting this stress increment in the principle of virtual work, as given in (81), leads to

$$\mathbf{Q}_a^{\mathrm{M}} = \int_{\Omega_{\mathrm{M}}} \mathbf{B}_a^{\mathrm{T}} \left[\mathbf{M}^{\mathrm{sec}} \Delta\varepsilon - K_2 \sigma'_n - 3k_{\mathrm{M}} \alpha_{\mathrm{M}} (\Delta T) \mathbf{I} \right] \mathrm{d}\Omega. \tag{94}$$

Performing once again the discretisation of the incremental strain field $\Delta\varepsilon$ in accordance to (90) and accounting for relation (94) leads to

$$\mathbf{Q}_a^{\mathrm{M}} = \sum_{b=1}^{NE} \left(\int_{\Omega_{\mathrm{M}}} \mathbf{B}_a^{\mathrm{T}} \mathbf{M}^{\mathrm{sec}} \mathbf{B}_b \mathrm{d}\Omega \right) \Delta\mathbf{u}_b \tag{95}$$

$$- K_2 \int_{\Omega_{\mathrm{M}}} \mathbf{B}_a^{\mathrm{T}} \sigma'_n \mathrm{d}\Omega - 3k_{\mathrm{M}} \alpha_{\mathrm{M}} (\Delta T) \int_{\Omega_{\mathrm{M}}} \mathbf{B}_a^{\mathrm{T}} \mathbf{I} \mathrm{d}\Omega, \tag{96}$$

or, written in a compacted form,

$$\mathbf{Q}_a^{\mathrm{M}} = \mathbf{0} = \sum_{b=1}^{NE} \mathbf{k}_{ab}^{\mathrm{M}} \Delta\mathbf{u}_b - \Delta\mathbf{f}_a^{\mathrm{M}}. \tag{97}$$

The previous expression is the generic equilibrium system of equations of a finite element of matrix material, where

$$\mathbf{k}_{ab}^{\mathrm{M}} = \int_{\Omega_{\mathrm{M}}} \mathbf{B}_a^{\mathrm{T}} \mathbf{M}^{\mathrm{sec}} \mathbf{B}_b \mathrm{d}\Omega \tag{98}$$

and

$$\Delta\mathbf{f}_a^{\mathrm{M}} = K_2 \int_{\Omega_{\mathrm{M}}} \mathbf{B}_a^{\mathrm{T}} \sigma'_n \mathrm{d}\Omega + 3k_{\mathrm{M}} \alpha_{\mathrm{M}} (\Delta T) \int_{\Omega_{\mathrm{M}}} \mathbf{B}_a^{\mathrm{T}} \mathbf{I} \mathrm{d}\Omega \tag{99}$$

are the stiffness matrix and the second member for the matrix material finite elements, respectively.

According to the previously described formulations and considering the element equilibrium equation systems (92) and (97), the global system of equations that must be solved is

$$\mathbf{Q}^{\mathrm{R}} + \mathbf{Q}^{\mathrm{M}} = \mathbf{0}. \tag{100}$$

This system of equations can still be solved as

$$\sum_{B=1}^{NN} \mathbf{K}_{AB} \Delta \mathbf{u}_{\mathrm{B}} = \Delta \mathbf{F}_{\mathrm{A}} \tag{101}$$

where $\mathbf{K}_{AB}$ is the global stiffness matrix, $\Delta \mathbf{u}_{\mathrm{B}}$ is the increment displacement vector at the current time instant and $\Delta \mathbf{F}_{\mathrm{A}}$ is the global second member vector. A and B designate the global numbering of the nodes in the finite element mesh.

2.4 Time-Step Optimisation

The constitutive equations described in previous sections, relative to the matrix material, are highly non-linear. As a consequence, using a constant time-step size can be an inadequate approach to obtain good numerical results. Doing so, the time-step should be sufficiently small to guarantee the stability of the numerical approach during the whole process simulation. Thus, it is of utmost importance to use a variable time-step size algorithm when implementing the formulations described [35].

The progressive gradient integration method is relatively simple to implement due to the fact that it is not necessary to iterate to determine the state variables on each increment. However, when rapid changes in the plastic strain rate occur, the results obtained with the progressive gradient integration method can become inaccurate. Nonetheless, this problem can be minimised by implementing an additional and complementary algorithm to automatically control the time-step size on each increment. The proposed control algorithm is based on the variations of the plastic strain rate.

The control parameter in this automatic time-step algorithm is the maximum increment of plastic strain in all the integration points of the finite element discretisation during the current time increment. Two distinct criteria are defined in order to do so. The first criterion is based on r_C, which is the parameter that controls the variations on the equivalent plastic strain rate, that is,

$$r_C = \frac{C_{\max}}{C_{\mathrm{tol}}} \quad \text{with} \quad C_{\max} = \max_{i=1,ng} \left| \dot{\bar{\varepsilon}}^{\mathrm{p}}_{i,n+1} - \dot{\bar{\varepsilon}}^{\mathrm{p}}_{i,n} \right| \tag{102}$$

where $C_{\max}$ is the maximum equivalent plastic strain rate variation in the current time increment among all the integration Gauss points. C_{tol} is a predefined (user-defined) control parameter that can be determined as

$$C_{\mathrm{tol}} = \delta \frac{s_0}{E_{\mathrm{M}}}. \tag{103}$$

ng and $\delta \in]0, 1]$ on the previous relations are the total number of Gauss points of the domain and a scalar parameter, respectively. E_{M} and s_0 are the elastic modulus and the initial value of the state variable s, respectively.

The second criterion limits the equivalent plastic strain rate increment directly in such a way as to avoid too large plastic strain increments. To achieve this r_D is defined as

$$r_D = \frac{D_{\max}}{D_{\text{tol}}} \quad \text{with} \quad D_{\max} = \max_{i=1,ng} \Delta\bar{\varepsilon}_i^{\text{p}} \tag{104}$$

where D_{tol} is a predefined (user-defined) control parameter.

Based on the previously defined criteria, it is now possible to choose the dominant criterion, calculating the parameter $r_{\max} = max\{r_C, r_D\}$ and determining if the solution from the current increment is acceptable or not, modifying the time-step size whenever needed.

In order to perform this optimisation automatically it is possible to use an algorithm in which each increment is optimised for the following increment. The parameters that control this optimisation algorithm are the scalars $w_0 < 1$, $w_i > 1$ and $q_j < 1$ with $i = 1, \ldots, n$. If these parameters are chosen correctly it is possible to reach a compromise between total CPU simulation of the process and the precision of the obtained results.

With the proposed time step optimisation algorithm it is possible to adjust the increment size to be small in the stages where strong gradients are developed and to be large enough when the strain rate does not change significantly. Scalar values q_i define a finite set of intervals in which the correction factors w_i are applied, with $i = 1, \ldots, n$. Additionally, it is even possible to develop a continuous step optimisation process, performing a numerical fitting to the set of values (q_i, w_i). The following generic equation leads to the referred numerical adjustment and to the generation of several optimisation profiles controlling only the scalar parameter F_{c}

$$w = w_1 + (w_n - w_1)\left\{\frac{exp\left(F_{\text{c}}\,\frac{r_{\max} - q_1}{q_n - q_1}\right)}{exp(F_{\text{c}}) - 1}\right\}. \tag{105}$$

3 Implementation and Results

The models and approaches proposed in previous sections are now tested in the determination of residual stresses in specific metal matrix composite materials. For the sake of example, these models are tested using an Aluminium matrix composite, with SiC reinforcement.

It is natural to suppose that technological questions associated with the manufacturing of metal matrix composites (MMC) may influence their response in service within a particular structural application. Thus, it is of utmost importance and relevance to study and investigate the role of the manufacturing technological parameters on the final properties and characteristics of MMC and in particular on

the development and elimination of residual thermal stress fields. The particular aspects studied and presented on this section are: (1) the effect of the reinforcement volume fraction, F_{v}, on the final distribution of residual stresses and other state variables; and (2) the effect of the cooling rate, $\dot{T}$, on the levels of residual stresses. Other tecnological issues such as, for example, those related to the distribution, orientation, and morphology of the reinforcement are also very important and have been studied by other authors, such as Stautter et al. [48], Sorensen et al. [49], Watt et al. [50] and Pettermann et al. [51].

As an example of application of the models proposed and described in previous sections a set of numerical simulations was performed to test their the numerical efficiency. Results are shown concerning (1) the effect of the metal matrix composite reinforcement volume fraction and (2) the effect of the cooling rate. Numerical simulations are performed on a unidirectional fibre reinforced MMC. The geometrical model of this MMC and the corresponding representative unit cell are schematically represented in Fig. 2a, b, respectively.

Boundary conditions are such that the coordinate planes in the representative unit cell (RUC) are planes of symmetry. All finite element simulations were performed considering an Al-SiC composite. The material properties – elastic modulus, Lamé coefficients and CTE – for the aluminium matrix are temperature dependent and given as [14]

$$\begin{aligned} E_{\mathrm{M}}(T) &= 73474 - 43.48T[\mathrm{MPa}], \\ \mu_{\mathrm{M}}(T) &= 27041 - 17.057T[\mathrm{MPa}], \\ \alpha_{\mathrm{M}}(T) &= 28.7 \times 10^{-6} + 2.47 \times 10^{-8}T[\mathrm{K}^{-1}], \end{aligned} \tag{106}$$

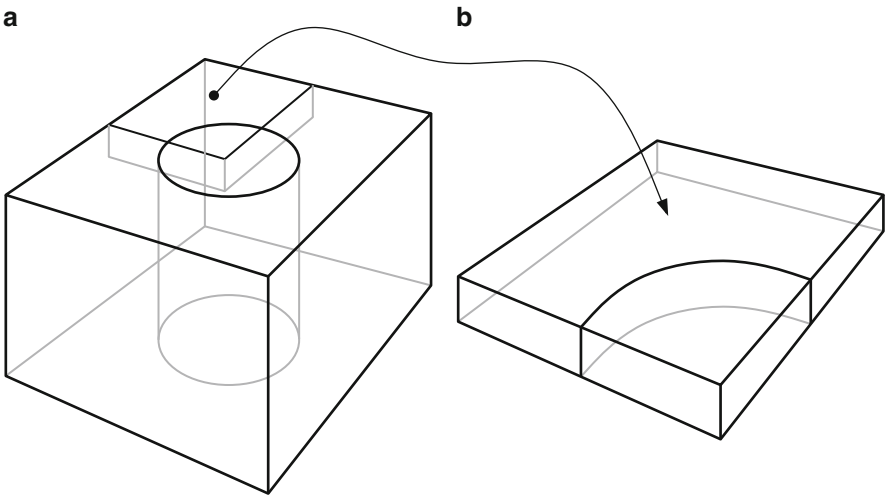

Fig. 2 Unidirectional fibre reinforced metal matrix composite (MMC): (**a**) geometrical model and (**b**) representative unit cell (RUC)

respectively, where T is the temperature in degrees Kelvin. The elastic modulus, Lamé coefficients and CTE for the reinforcement material are

$$\begin{aligned} E_{\mathrm{R}} &= 41 \times 10^4\,\mathrm{MPa}, \\ \mu_{\mathrm{R}} &= 16.532 \times 10^4\,\mathrm{MPa}, \\ \alpha_{\mathrm{R}} &= 0.43 \times 10^{-5}\,\mathrm{K}^{-1}, \end{aligned} \tag{107}$$

respectively. Material parameters used in the constitutive model are given by Tei-xeira-Dias and Menezes [14]. A constant cool rate is considered in all simulations and the resulting homogeneous temperature field is given by

$$T(t) = T_{\mathrm{i}} + \dot{T}t, \tag{108}$$

where t is the time. The initial and final temperatures are $T_{\mathrm{i}} = 933$ K and $T_{\mathrm{f}} = 293$ K, respectively.

3.1 Reinforcement Volume Fraction

The reinforcement volume fraction F_{v} is one of the manufacturing and technological parameters that influences most the mechanical and thermal characteristics of the composite material [26, 29, 52, 53]. Thus, the study of the influence of this parameter is particularly interesting as it can be defined and controlled both on the design and on the manufacturing stages in such a way as to achieve a set of desired mechanical properties for the MMC.

Numerical simulations were made on the referred representative unit cell using the constitutive models and numerical approaches described on previous sections. The σ_{xx} and σ_{yy} stress profiles along Oy are shown in Figs. 3 and 4 for reinforcement volume fractions in the range of 5–35%. A constant cooling rate $|\dot{T}| = 100\ \mathrm{Ks}^{-1}$ was considered. These results concern a representative unit cell (RUC) of a unidirectional fibre metal matrix composite, such as the one represented in Fig. 2. Directions Ox and Oy are the length and width of the RUC.

As expected, both the σ_{xx} and the σ_{yy} stress components are compressive within the reinforcement material and correspond to an hydrostatic stress state. It can also be observed that the compressive levels of σ_{xx} in the reinforcement decrease for increasing volume fraction. The same tendency can be observed for σ_{yy}. However, the levels of σ_{xx} increase with the volume fraction, that is, as the distance between reinforcement elements decreases. It can be seen that the equivalent stress that arises from the results presented is almost independent of the reinforcement volume fraction, reaching its maximum values near the matrix-reinforcement interface. The maximum value of the equivalent stress is close to 70 MPa at room temperature. This value is above the yield stress of the matrix material, which is close to 40 MPa.

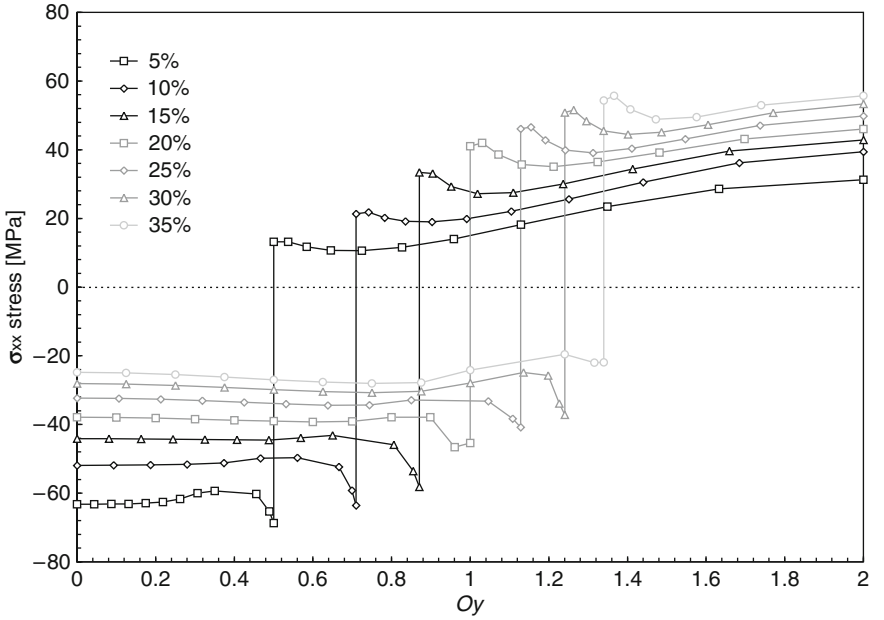

Fig. 3 σ_{xx} stress profiles along Oy for reinforcement volume fractions in the range of 5–35% at a constant cooling rate $|\dot{T}| = 100\ \mathrm{Ks}^{-1}$

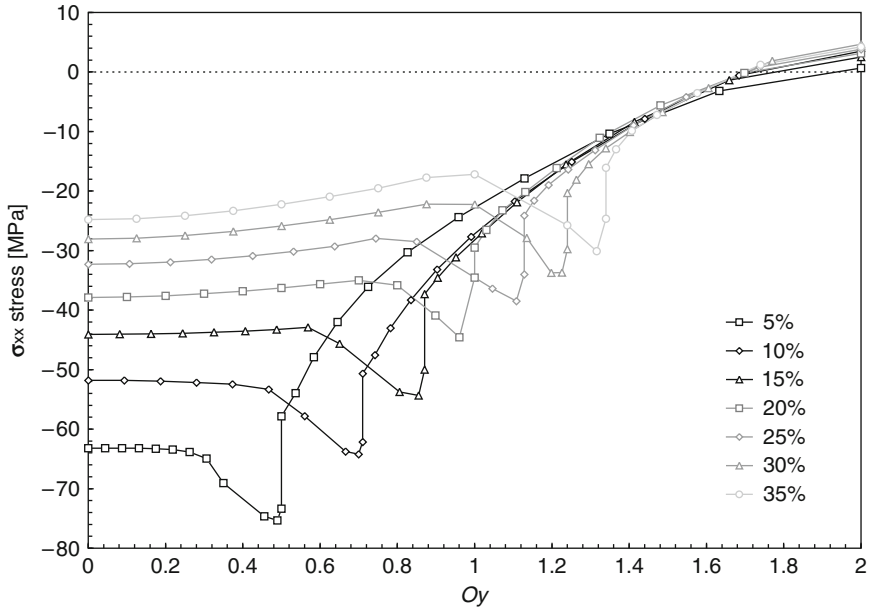

Fig. 4 σ_{yy} stress profiles along Oy for reinforcement volume fractions in the range of 5–35% at a constant cooling rate $|\dot{T}| = 100\ \mathrm{Ks}^{-1}$

This fact reflects the presence of hardening effects during the cooling down stages of the manufacturing process, as a consequence of the development of plastic strain.

3.2 Cooling Rate

As was stated before, most of the manufacturing processes used in the production of metal matrix composites (MMC) induce high temperature levels and gradients in the metallic matrix, often close to (or even above) its melting temperature. During the posterior cooling down stage, residual stresses may arise due to the mismatch between the coefficients of thermal expansion (CTE) of the constituent materials. Consequently, the cooling down stage is expected to have a determinant effect on the levels of residual stresses at room temperature within the MMC. Absolute cooling rates in the range of 0.1 to 500 Ks^{-1} were tested considering that the material is stress-free at fabrication temperature (T_i). The dependence of the equivalent stress σ_eq, internal parameter s and equivalent plastic strain $\dot{\bar{\varepsilon}}^\mathrm{p}$ on the cooling rate are shown in Fig. 5.

In these results it can be clearly observed that there is a gradual decrease of both σ_eq and s with $|\dot{T}|$ and also that this effect increases for absolute cooling rates below

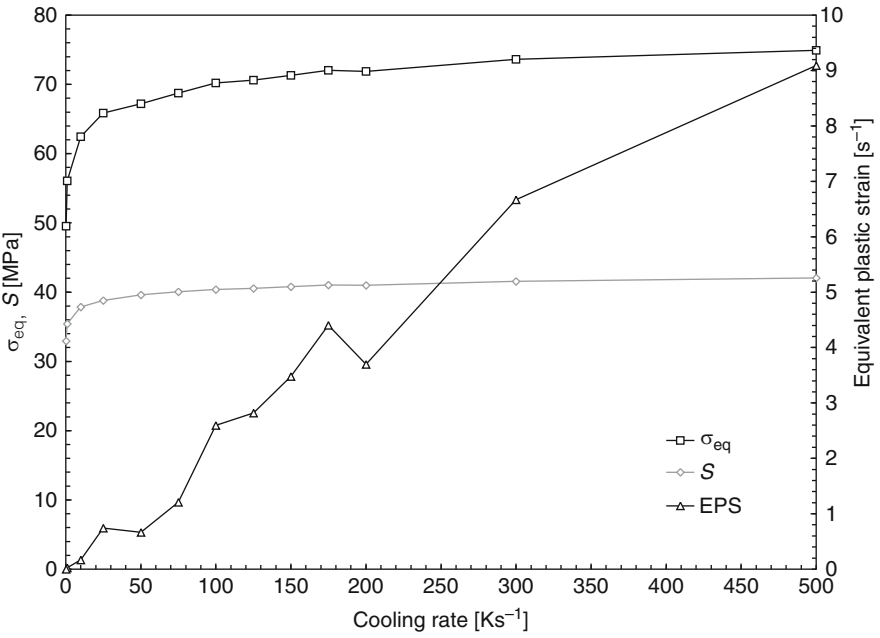

Fig. 5 Dependence of the equivalent stress σ_{eq}, state variable s and equivalent plastic strain $\dot{\bar{\varepsilon}}^\mathrm{p}$ on the cooling rate $(\dot{T})$

50 Ks^{-1}. Nonetheless, in global terms, it can be stated that the cooling rate has a limited effect on the residual stress levels at room temperature. The effect of changing the cooling rate is mostly felt on the relatively low stresses generated at higher temperatures.

4 Final Remarks

The authors presented a full numerical approach to the determination of residual stresses in dual-phase microstructured materials, with applications to metal matrix composites (MMC). The model is applied in a finite element algorithm and tested with some numerical examples in order to prove its effectiveness and evaluate the effect of the reinforcement volume fraction and of the cooling rate on the levels of residual stresses at room temperature. Residual stress fields are determined in a representative unit cell (RUC) associated with a unidirectional fibre reinforced Al-SiC composite with volume fractions ranging from 5 to 35%.

It is shown that both normal stress components σ_{xx} and σ_{yy} are compressive in nature resulting in a hydrostatic stress state in the reinforcement. The levels of compressive stress decrease for the higher volume fractions. Nonetheless, the tendency is opposite in the metallic matrix with higher values of σ_{xx} for increasing reinforcement volume fractions. The equivalent stress reaches values above the yield limit, leading to the development of plastic strain near the matrix-reinforcement interface.

The influence of the cooling rate on the residual stresses at room temperature is not evident. This influence is only significant for absolute cooling rates under 50 Ks^{-1}. This can be explained by the fact that the residual stresses at room temperature are mostly generated at the lower temperature range, that is, under 600 K, where the viscoplastic behaviour of the aluminium matrix is less sensitive to the strain rate.

References

1. Parlevliet, P.P., Bersee, H.E.N., Beukers, A.: Residual stresses in thermoplastic composites – a study of the literature – Part I: Formation of residual stresses. Compos. Part A **37**(11), 1847–1857 (2006)
2. Parlevliet, P.P., Bersee, H.E.N., Beukers, A.: Residual stresses in thermoplastic composites – a study of the literature – Part II: Experimental techniques. Compos. Part A **38**(3), 651–665 (2006)
3. Liu, H.T., Sun, L.Z.: Effects of thermal residual stresses on effective elastoplastic behavior of metal matrix composites. Int. J. Solids Struct. **41**(8), 2189–2203 (2004)
4. Meijer, G., Ellyin, F., Xia, Z.: Aspects of residual thermal stress/strain in particle reinforced metal matrix composites. Compos. Part B **31**(1), 29–37 (2000)
5. Huang, Z.-M.: Cyclic response of metal matrix composite laminates subjected to thermo-mechanical fatigue loads. Int. J. Fatigue **24**, 463–475 (2002)

6. Gungor, S.: Residual stress measurements in fibre reinforced titanium alloy composites. Acta Mater. **50**(8), 2053–2073 (2002)
7. Altan, G., Topcu, M.: Thermo-elastic stress of a metal-matrix composite disc under linearly-increasing temperature loading by analytical and FEM analysis. Adv. Eng. Softw. **41**(4), 604–610 (2010)
8. Rudajevova, A., Milicka, K.: Residual and thermal strain in AX41 magnesium alloy reinforced with short Saffil fibres. Compos. Sci. Technol **68**(12), 2474–2478 (2008)
9. Sayman, O.: An elastic-plastic thermal stress analysis of aluminum metal-matrix composite beams. Compos. Struct. **53**(4), 419–425 (2001)
10. Sayman, O., Ozer, M.R.: Elastic-plastic thermal stress analysis of aluminum-matrix composite beams under a parabolically temperature distribution. Compos. Sci. Technol. **61**(14), 2129–2137 (2001)
11. Zhang, H., Ramesh, K.T., Chin, E.S.C.: A multi-axial constitutive model for metal matrix composites. J. Mech. Phys. Solids **56**(10), 2972–2983 (2008)
12. Ju, D.-Y.: Simulation of the thermo-mechanical and interfacial stress of metal matrix composites under thermal shock process. Compos. Struct. **48**, 113–118 (2000)
13. Choo, H., Bourke, M.A.M., Daymond, M.R.: A finite-element analysis of the inelastic relaxation of thermal residual stresses in continuous-fibre-reinforced composites. Compos. Sci. Technol **61**(12), 1757–1772 (2001)
14. Teixeira-Dias, F., Menezes, L.F.: Numerical determination of the influence of the cooling rate and reinforcement volume fraction on the levels of residual stresses in Al-SiC composites. Comput. Mater. Sci. **21**(1), 26–36 (2001)
15. Teixeira-Dias, F., Andrade-Campos, A., Pinho-da-Cruz, J.: On the effect of the orientation of the reinforcement on the overall behaviour of Al-SiC_p composites. Comput. Struct. **82**, 1323–1331 (2004)
16. Ledbetter, H.M., Austin, M.W.: Internal strain (stress) in an SiC–Al particle-reinforced composite: an X-ray diffraction study. Mater. Sci. Eng. **89**, 53–61 (1987)
17. Kolhe, R., Hui, C.Y., Ustundag, E., Sass, S.L.: Residual thermal stresses and calculation of the critical metal particle size for interfacial crack extension in metal-ceramic matrix composites. Acta Mater. **44**(1), 279–287 (1996)
18. Fernandez, P., Fernandez, R., Gonzalez-Doncel, G., Bruno, G.: Correlation between matrix residual stresses and composite yield strength in PM 6061-Al-15 vol.% SiC_w. Scripta Mater. **52**(8), 793–797 (2004)
19. Jiang, Z., Li, G., Lian, J., Ding, X., Sun, J.: Elastic-plastic stress transfer in short fibre-reinforced metal-matrix composites. Compos. Sci. Technol. **64**, 1661–1670 (2004)
20. Fang, Q., Sidky, P.S., Hocking, G.M.: Residual stresses in titanium matrix composites (TMC) in thermomechanical cycling using matrix etching. Mater. Sci. Eng. **288**(2), 293–297 (2000)
21. Bruno, G., Fernandez, R., Gonzalez-Doncel, G.: Relaxation of the residual stress in 6061 Al-15 vol.% SiC_w composites by isothermal annealing. Mater. Sci. Eng. **382**, 188–197 (2004)
22. Michel, J.C., Suquet, P.: An analytical and numerical study of the overall behaviour of metal-matrix composites. Model. Simulat. Mater. Sci. Eng. **2**(3A), 637–658 (1994)
23. Ramakrishnan, N.: An analytical study on strengthening of particulate reinforced metal matrix composites. Acta Mater. **44**(1), 69–77 (1996)
24. Shen, Y.-L., Finot, M., Needleman, A., Suresh, S.: Effective elastic response of two-phase composites. Acta Mater. **42**(1), 77–97 (1994)
25. Zahl, D.B.: The effect of interfacial sliding on the strength of metal matrix composites. Comput. Mater. Sci. **1**(3), 249–258 (1993)
26. Ho, S., Saigal, A.: Thermal residual stresses and mechanical behavior of cast SiC/Al composites. Mater. Sci. Eng. A **183**, 39–47 (1994)
27. Shaw, L.L., Miracle, D.B.: Effects of an interfacial region on the transverse behavior of metal-matrix composites – a finite element analysis. Acta Mater. **44**(5), 2043–2055 (1996)
28. Anand, L.: Constitutive equations for hot-working of metals. Int. J. Plast. **1**(3), 213–231 (1985)

29. Shen, Y.-L., Finot, M., Needleman, A., Suresh, S.: Effective plastic response of two-phase composites. Acta Mater. **43**(4), 1701–1722 (1995)
30. Suéry, M., Teodosiu, C., Menezes, L.F.: Thermal residual stresses in particle-reinforced viscoplastic metal matrix composites. Mater. Sci. Eng. A **167**, 97–105 (1993)
31. Hughes, T.J.R.: Numerical implementation of constitutive models: rate independent deviatoric plasticity, theoretical foundations for large scale computations of nonlinear material behaviour. Martinus Nighoff, The Netherlands (1994)
32. Zywicz, E., Parks, D.M.: Thermo-viscoplastic residual stresses in metal matrix composites. Compos. Sci. Technol. **33**(4), 295–315 (1988)
33. Brown, S.B., Kim, K.H., Anand, L.: An internal variable constitutive model for hot working of metals. Int. J. Plast. **5**(2), 95–130 (1989)
34. Kocks, U.F., Argon, A.S., Ashby, M.F.: Thermodynaics and kinetics of slip. Pergamon, Oxford (1975)
35. Lush, A.M., Weber, G., Anand, L.: An implicit time-integration procedure for a set of internal variable constitutive equations for isotropic elasto-viscoplasticity. Int. J. Plast. **5**(5), 521–549 (1989)
36. Weber, G., Anand, L.: Finite deformation constitutive equations and a time integration procedure for isotropic, hyperelastic-viscoplastic solids. Comput. Methods Appl. Mech. Eng. **79**(2), 173–202 (1990)
37. Weber, G., Lush, A.M., Zavaliangos, A., Anand, L.: An objective time-integration procedure for isotropic rate-independent and rate-dependent elastic-plastic constitutive equations. Int. J. Plast. **6**(6), 701–744 (1990)
38. Teixeira-Dias, F., Menezes, L.F.: A kinematic and incremental integration model for the micromechanical numerical analysis of dual-phase materials. Comput. Mater. Sci. **25**, 237–245 (2002)
39. Pierce, D., Shih, C.F., Needleman, A.: A tangent modulus method for rate dependent solids. Comput. Struct. **18**(5), 875–887 (1984)
40. Dhatt, G., Touzout, G.: The finite element method displayed. Wiley, New York (1984)
41. Hughes, T.J.R.: The finite element method – linear static and dynamic finite element analysis. Prentice-Hall, Englewood Cliffs (1987)
42. Nagtegaal, J.C., Parks, D.M., Rice, J.R.: On numerically accurate finite element solutions in the fully plastic range. Comput. Methods. Appl. Mech. Eng. **4**(2), 153–177 (1974)
43. Takizawa, H., Makinouchi, A., Santos, A., Mori, N.: FE-Simulation of 3D Sheet Metal Forming Processes in Automotive Industry, VDI Berichte, vol 894, pp 167–184. VDI Verlag (1991)
44. Malkus, D.S., Hughes, T.J.R.: Mixed finite element methods – reduced and selective integration techniques: a unification of concepts. Comput. Methods Appl. Mech. Eng. **15**(1), 63–81 (1978)
45. Hughes, T.J.R.: Generalization of selective integration procedures to anisotropic and nonlinear media. Int. J. Numer. Methods Eng. **15**(9), 1413–1418 (1980)
46. Shimodaira, H.: Equivalence between mixed models and displacement models sing reduced integration. Int. J. Numer. Methods Eng. **21**(1), 89–104 (1985)
47. Menezes, L.F., Teodosiu, C., Makinouchi, A.: FE-Simulation of 3D Sheet Metal Forming Processes in Automotive Industry, VDI Berichte, vol 894, pp 381–403. VDI Verlag (1991)
48. Sautter, M., Dietrich, Ch, Poech, M.H., Schmauder, S., Fischmeister, H.F.: Finite element modelling of a transverse-loaded fibre composite effects of section size and net density. Comput. Mater. Sci. **1**(3), 225–233 (1993)
49. Sorensen, N.J., Suresh, S., Tvergaard, V., Needleman, A.: Effects of reinforcement orientation on the tensile response of metal-matrix composites. Mater. Sci. Eng. A **197**(1), 1–10 (1995)
50. Watt, D.F., Xu, X.Q., Lloyd, D.J.: Effects of particle morphology and spacing on the strain fields in a plastically deforming matrix. Acta Mater. **44**(2), 789–799 (1996)

51. Pettermann, H.E., Boehm, H.J., Rammerstorfer, F.G.: Some direction-dependent properties of matrix-inclusion type composites with given reinforcement orientation distributions. Compos. Part B **28**(3), 253–265 (1997)
52. Jain, M., MacEwen, S.R., Wu, L.: Finite element modelling of residual stresses and strength differential effect in discontinuously reinforced metal matrix composites. Mater. Sci. Eng. A **183**(1–2), 111–120 (1994)
53. Manoharan, M., Gupta, M.: Effect of silicon carbide volume fraction on the work hardening behaviour of thermomechanically processed aluminium-based metal matrix composites. Compos. Part B **30**(1), 107–112 (1999)

http://www.springer.com/978-3-642-04402-1

Heat Transfer in Multi-Phase Materials
Öchsner, A.; Murch, G.E. (Eds.)
2011, XI, 460 p., Hardcover
ISBN: 978-3-642-04402-1